Ultramicroscopy 159 (2015) 34–45

Contents lists available at ScienceDirect

Ultramicroscopy

journal homepage: www.elsevier.com/locate/ultramic

Surface effects on mean inner potentials studied using density functional theory

Robert S. Pennington [a,*], Chris B. Boothroyd [b], Rafal E. Dunin-Borkowski [b]

[a] Institute for Experimental Physics, Ulm University, Albert-Einstein-Allee 11, 89081 Ulm, Germany
[b] Ernst Ruska-Centre and Peter Grüneberg Institute, Forschungzentrum Jülich, 52425 Jülich, Germany

ARTICLE INFO

Article history:
Received 21 April 2015
Received in revised form
22 July 2015
Accepted 26 July 2015
Available online 29 July 2015

Keywords:
Electron holography
Mean inner potential
Surface reconstruction
Density functional theory

ABSTRACT

Quantitative materials characterization using electron holography frequently requires knowledge of the mean inner potential, but reported experimental mean inner potential measurements can vary widely. Using density functional theory, we have simulated the mean inner potential for materials with a range of different surface conditions and geometries. We use both "thin-film" and "nanowire" specimen geometries. We consider clean bulk-terminated surfaces with different facets and surface reconstructions using atom positions from both structural optimization and experimental data and we also consider surfaces both with and without adsorbates. We find that the mean inner potential is surface-dependent, with the strongest dependency on surface adsorbates. We discuss the outlook and perspective for future mean inner potential measurements.

1. Introduction

The amplitude and phase of the electron beam in the transmission electron microscope are directly accessible using electron holographic techniques [1–3]. The sensitivity of the electron phase to electric and magnetic potentials has been used for quantitative micro- and nano-scale materials characterization on a wide variety of specimens [4–10]. However, quantification of phase shifts inside material relative to free space relies on knowing the material's mean inner potential V_0 [3]. V_0, defined as the mean electrostatic potential difference in a material relative to free space far from the material, is related to the zero-scattering-angle electron scattering factor and diamagnetic susceptibility [11,12,3]. For a single material, measurements of V_0 performed by different groups do not necessarily agree [13], so density functional theory (DFT) calculations have been used previously to attempt to predict V_0 [14]. Because an infinite crystal with no surfaces has no external reference point to use for an electrostatic potential and thus no definable mean inner potential [15], surfaces must be present for V_0 to be defined, but rarely has the effect of the surface been explicitly considered in these DFT calculations [16,17], especially systematically or explicitly.

Experimental V_0 measurements using off-axis electron holography started soon after the development of the electrostatic biprism [2], with attempts in the 1950s to measure V_0 for carbon [18], gold, and other materials [4]. Continued interest has led to electron holographic V_0 measurements for many materials, including semiconductors such as silicon [19–21,14], germanium [22] and group III–V materials [23,14]. Other non-holographic methods, such as electron diffraction, have also been used for mean inner potential determination on materials such as diamond, silicon, germanium, and metals [24–26].

However, as previously noted [26,14], these measurements often do not agree with each other, or have large margins of error. Kruse et al. [14] cite four compounds with more than one reported V_0 measurement (Si, Ge, GaAs, and InP), and, in all four cases, at least one measurement disagrees with the others. For germanium, an evaporation-based "wet" preparation determined 15.6 ± 0.8 V [27], and a cleaved (110) wedge found 14.3 ± 0.2 V [22]. For crystalline silicon, V_0 has been measured to be 9.26 ± 0.08 V from (111)-cleaved wedges [19], 12.1 ± 1.3 V from oxide-covered Si nanospheres [20], 11.5 ± 0.5 V from crushed bulk Si [21], and 12.52 ± 0.71 V from (110)-cleaved wedges [14]; we note that the first of these silicon values is much lower than the following three measurements. Even if only the latter three silicon values are considered, this provides a wide range of possible V_0 values with large margins of error. There are possible experimental explanations for these discrepancies, including dynamical diffraction [19,28] and anomalies for V_0 measurements of small nanoparticles were attributed to size-dependent strain [29], as well as specimen charging and inaccurate thickness determination. Thus, to establish V_0 benchmark values with higher precision, simulations have proven useful.

V_0 can be calculated from isolated-atom scattering factors

* Corresponding author.
E-mail address: robert.pennington@uni-ulm.de (R.S. Pennington).

http://dx.doi.org/10.1016/j.ultramic.2015.07.011
0304-3991/

(IASF), or simulated using *ab initio* methods like density functional theory (DFT). The IASF approach has the advantage of being notably faster, simply requiring tabulated electron scattering factors [12,30] calculated for isolated atoms. However, IASF neglects chemical bonding, which has a notable effect [14]. DFT is more realistic, and includes chemical bonding, exchange, and correlation effects, but DFT exchange-correlation functionals also introduce some approximations [31]. DFT V_0 calculations previously reported include those of silicon, germanium, and MgO [16], wurtzite-structure group III–V semiconductors and gold [32], group II–VI semiconductors [33], zincblende-structure group-IV and group-III–V semiconductors [14], and multiple carbon allotropes (diamond, graphite, and amorphous carbon) [34].

Both different DFT programs, and different density functionals, can be used for V_0 simulation. In this work, we chose the GPAW code [35] because its use of grid-based projector-augmented wavefunctions in real-space [31,36] provides easy calculation of V_0 [17], and to compare with WIEN2k as used in [14]. We also use only the PBE (Perdew–Burke–Ernzerhof) exchange-correlation functional [37] to model electron–electron interactions, which is a common choice, including for V_0 calculation [14], but not the only choice (*e.g.* [16] uses the LDA (Local Density Approximation) exchange-correlation functional [31]). Different exchange-correlation functionals make different approximations for electron–electron interactions, and, thus, choosing a functional also chooses which approximations are made [31,37]; we discuss the effect of different functionals on V_0 in Appendix A.

Surface effects on electron-holographic measurements of V_0 have been briefly considered previously. Saldin and Spence in [38] discussed the theoretical influence of the Fermi level and the work function on V_0. According to their formulation, changes to the work function should lead to changes in the mean inner potential. For DFT-simulated V_0, Kim et al. [16] briefly consider the effect of different bulk-terminated surfaces, but for only a few cases. Our previous DFT simulation work, in [17], also considers only a few cases. This leads to the question of whether testing a range of surfaces and several materials in-depth would show a surface-dependent V_0.

In this work, we consider the effect of the specimen surface on V_0 through DFT calculations for different specimen surface conditions, expanding on our previous work [17]. In Section 2, we present results from DFT simulation of the mean inner potential using the GPAW program [35], first determining what precision can be expected for V_0 simulations with GPAW, then testing "thin-film" cases for quantitative V_0 simulations and "nanowire" cases to further explore and explain the surface effects seen in the thin-film simulations. Finally, in Sections 3 and 4, we discuss these results, and provide some guidance for future mean inner potential measurements.

2. Results

In this section, we report the results of our DFT calculations of the mean inner potential (V_0). Our DFT simulations use the GPAW code [35] (version 0.6 stable) and its dependency, the Atomic Simulation Environment (version 3.2.0 stable) [39], and experimental lattice parameters are from the literature [40,41]. Generating V_0 requires summing the electrostatic potential over a volume. As previously reported [17], we sum the grid-based pseudo-Hartree electrostatic potential in that volume combined with the electrostatic-correction function's set of scalars for each atom inside that volume, where the electrostatic corrections are calculated for the core electrons of each atom using the known PAW atomic setups and the unit-cell volume.

We use both "thin-film" and "nanowire" specimen geometries

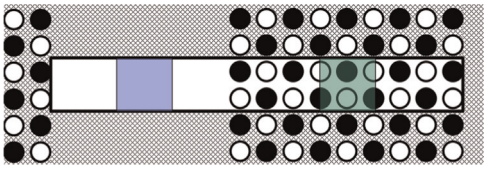

Fig. 1. Thin-film simulation geometry for a (110) surface, projected along the $\hat{x}$-axis. The black-outlined, non-crosshatched area is the specimen geometry input into the program, with both specimen and vacuum regions. The crosshatched area represents the effect of infinite periodic boundary conditions. V_0 is calculated by subtracting the average electrostatic potential over the middle unit cell of the specimen (green) from an equivalent volume in the middle of vacuum (blue). Note that the geometry seen here is also periodic in the direction normal to the page. (For interpretation of the references to color in this figure caption, the reader is referred to the web version of this paper.)

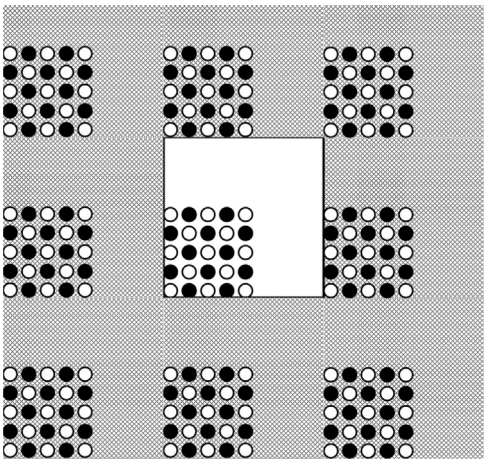

Fig. 2. Nanowire simulation geometry, projected along the $\hat{x}$-axis. As with Fig. 1, the crosshatched area represents the effect of periodic boundary conditions. The nanowires are infinitely long in the direction normal to the page.

in our simulations. Shown in Fig. 1, a "thin-film" specimen has surfaces in the $\hat{z}$ direction, and material extending infinitely in the $\hat{y}$ and $\hat{x}$ directions, like an infinite thin film. This is the approach that has been reported previously for V_0 calculation. We also introduce a "nanowire" specimen, not previously reported. Shown in Fig. 2, a "nanowire" specimen has surfaces in the $\hat{z}$ and $\hat{y}$ directions, and material extending infinitely in the $\hat{x}$ direction, like an infinitely long nanowire. In both cases, periodic boundary conditions are used in all three directions, so the thin-film simulation simulates an infinite stack of thin-films, and the nanowire simulation simulates an infinite array of nanowires. The distances between the surfaces of different objects are chosen to avoid interaction effects between different thin films or nanowires.

First, we discuss the accuracy and precision of V_0 simulated using our chosen DFT code, GPAW, and compare it to the WIEN2k code in [14]. However, we must then discuss DFT-generated minimum-energy lattice parameters. These sections establish a "baseline" for V_0, using (110) bulk-terminated surfaces.

Second, we present the results for V_0 simulated from different surface states. For clean surfaces, we examine bulk-terminated and surface-reconstruction states, with surface reconstructions either from the literature or using DFT structural optimization. For surfaces with adsorbates, we consider first experimental adsorbate states, but we focus on structurally optimized adsorbate configurations. These specific adsorbate configurations are not necessarily experimentally achievable, but they are used to provide insight into surface effects on V_0.

Third, to help explain the surface dependence we see, we present the results of "nanowire" simulations. The nanowire simulations display fringing fields, as expected, which helps explain